Attractor Reconstruction and Fractal Dimension for Actual Neuron Signals

Yoko Uwate†, Martin Schüle‡, Thomas Ott‡ and Yoshifumi Nishio†
†Dept. of Electrical and Electronic Engineering, Tokushima University
2-1 Minami Josanjima, Tokushima 770-8506, Japan
Tel: +81-88-656-7662, Fax: +81-88-656-7471
Email: {uwate, nishio}@ee.tokushima-u.ac.jp
‡Institute of Computational Life Sciences, Zurich University of Applid Sciences
Schloss, Wädenswil 8820, Switzerland
Email: {scli, ottt}@zhaw.ch

***Abstract*—In this study, we investigate complexities of actual neuron signals using nonlinear time series analysis such as attractor reconstruction and fractal dimension. The simulation results showed that changes in the chaotic characteristics obtained from attractor reconstruction and the graphs of fractal dimensions as the brain developed.**

I. Introduction

Understanding how neural circuits in the brain are formed and function is a major goal of many neuroscience projects [1]. Neurons fire and generate spikes due to the potential difference across ion channels inside and outside the cell. Neuronal signals that generate continuous spike sequences are referred to as being in a burst state. In many studies of neuron activity patterns, the detection and analysis of these burst patterns are central because the correlation of these burst patterns is believed to play an important role in the brain's information processing, such as information transmission processes [2], [3]. While these analysis techniques are effective for investigating current brain activity patterns, they are too complex to observe the influence of the entire network of neuron groups. The applicant believes that new indicators and evaluation methods that can more simply evaluate the activity patterns of neuron groups are necessary.

In our previous study, we applied nonlinear time series analyses, including attractor reconstruction, recurrence plots, and Lyapunov exponents, to actual neuron data obtained from Wister rat brain [4]. Attractor reconstruction and recurrence plots successfully visualized the neuron signals, and the calculation of Lyapunov exponents confirmed that the neuron signals exhibit chaotic properties.

In this study, we extended the length of the time series analyzed from 1 minute to 3 minutes. Additionally, we investigated new features derived from attractor reconstruction images, focusing on two aspects: the incorporation of temporal information into two-dimensional attractors and the distribution of distances between plots in the two-dimensional attractor space. Furthermore, to clarify the chaotic nature of neuron signals, we examined not only Lyapunov exponents but also fractal dimensions, which were also computed. Simulation results revealed that new information from the attractors and graphs of fractal dimensions demonstrated changes in these characteristics as neurons developed.

II. Actual Neuron Data

The neuronal data used in this study are explained. Wister rat cortex was used as primary cell cultures. Embryonic day 18 rodent brains were taken from mother rats [5]. It was stored in an incubator and neuronal signals were measured 15, 20 and 30 days after taking it out. By using this neuron data, it becomes possible to understand the characteristics of chaotic properties during the brain's developmental process. The neuron signals were measured using MaxOne from MaxWell Biosystems [6], [7]. MaxOne is CMOS-based high-density micro electrode array (HD-MEA).

Figure 1shows the raster plot obtained from the same neuronal culture across multiple days; DIV15, 20 and 30, using 1,024 electrodes. DIV stands for Day in Vitro, where the numbers represent days. In other words, DIV15 means 15 days after the rat brain was picked out.

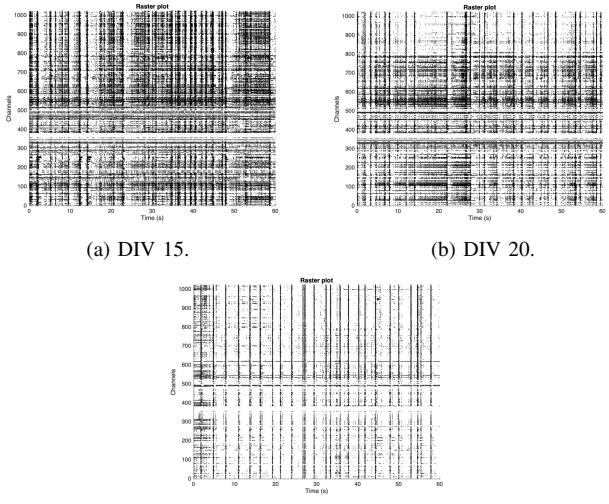

(a) DIV 15. (b) DIV 20.

(c) DIV 30.

Fig. 1. Raster plots.

Next, we calculate the spike rate at time bins, then time-series data are obtained as shown in Fig. 2.

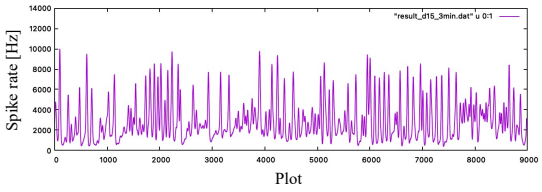

(a) DIV 15.

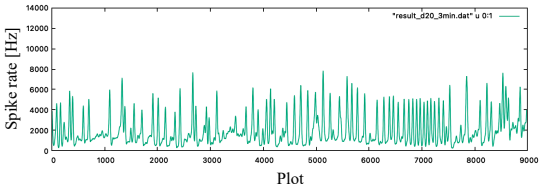

(b) DIV 20.

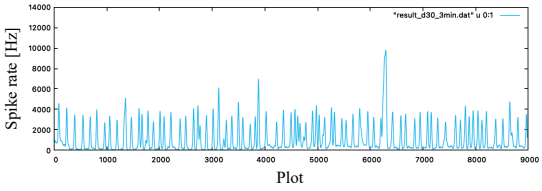

(c) DIV 30.

Fig. 2. Time series of spike rate.

III. Attractor Reconstruction

As a method for attractor reconstruction, the use of a time-delay coordinate system based on differences at fixed time delays has been proposed [8], [9]. The transformation into a time-delay coordinate system is performed by constructing an m-dimensional vector in a reconstructed state space of dimension m, using the following equation, where τ represents the time delay:

$$y(t) = \{x(t), x(t+\tau), ..., x(t+(m-1)\tau\}. \quad (1)$$

Figure 3 shows the simulation results when neuron time series data is embedded in 3-dimensional space with τ=10. From this figure, we confirm that all three cultures exhibit a clear structure, because the orbit draws in certain range and does not move about randomly. It was also found that the part of the attractor showing complex behavior became smaller as the number of days increased: at DIV 15, the entire attractor is complex, while at DIV 30, a mixture of complex and simple behavior can be observed.

The time series of the neuronal signals are embedded in a two-dimensional space and the results with the time information shown in color is shown in Fig. 4. Red indicates early time and blue indicates time passed. These results show that red and blue dots are mixed in the case of young culture (DIV 15), whereas red and blue dots are separated in the case of neuronal signals that have been old for a number of days (DIV 30).

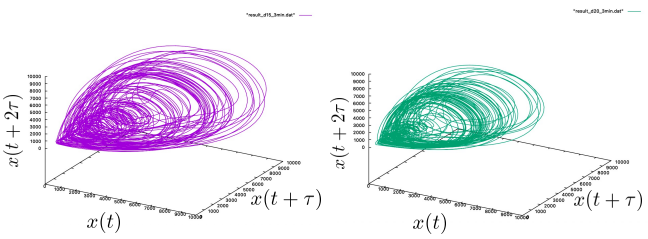

(a) DIV 15. (b) DIV 20.

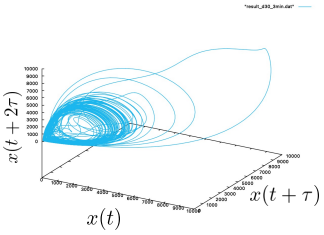

(c) DIV 30.

Fig. 3. Attractor reconstruction (τ=10).

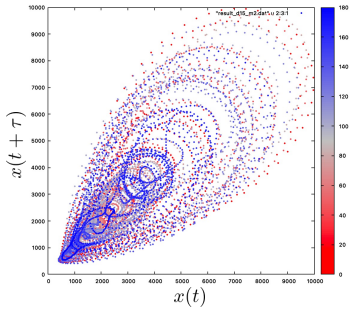

(a) DIV 15.

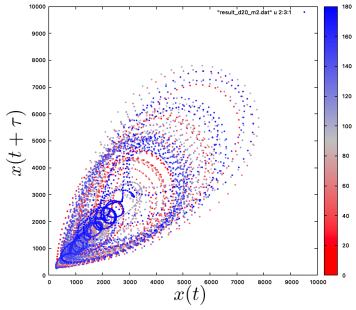

(b) DIV 20.

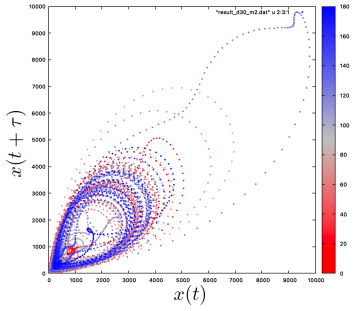

(c) DIV 30.

Fig. 4. Attractor reconstruction in 2-dimensional space with time information.

Next, in the diagram in Fig. 4, the distance between the two points is calculated and shown as a distribution in Fig. 5. In the case of DIV15, the distribution ranges widely from short to long distances. In the case of DIV20, there are two peaks in the distribution: one at distance 2 and the other at distance 25. In the case of DIV 30, the distance between the two peaks is smaller and, moreover, the peak below distance 1 is very large. The other peak is made at distance 19.

In summary, Figs. 3-5 show that young neurons are more complex and older neurons have grown to have some structure. Understanding the details of their structure is a future task.

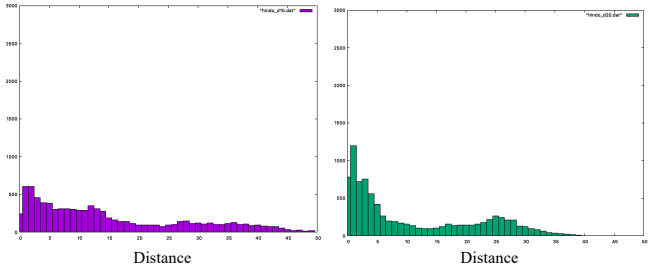

(a) DIV 15. (b) DIV 20.

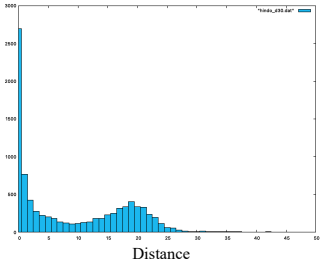

(c) DIV 30.

Fig. 5. Distribution of distance.

IV. Fractal Dimension

Finally, the fractal dimension is investigated for the neuronal signals. One feature of deterministic chaos is self-similarity as a static feature of attractors. This can be quantitatively evaluated by fractal dimension analysis. If the estimated fractal dimension for an attractor is non-integer, it is likely that the dynamical system that produced the attractor had chaotic dynamics.

In this study, the fractal dimension is obtained using the correlation integral method. This is called the GP (Grassberger-Procaccia) algorithm [10], [10]. The GP algorithm calculates the correlation dimension which is one measure of fractal dimension by calculating the correlation integral.

If $\mathbf{v}(i) \in \mathbf{R}^m$ is a point on the reconstructed attractor, the correlation integral is defined by the following equation.

$$C^m(r) = \lim_{n\to\infty} \frac{1}{N^2} \sum_{i,j=1}^{N} I(r - |\mathbf{v}(i) - \mathbf{v}(j)|. \qquad (2)$$

where $I(t)$ is Heaviside function as described by the following equation.

$$I(t) = \begin{cases} 1 & (t \geq 0) \\ 0 & (t < 0) \end{cases} \qquad (3)$$

A graph of the relationship between the logarithm of the correlation integral and distance when the embedding dimension m is varied from 2 to 10 is shown in Fig. 6.

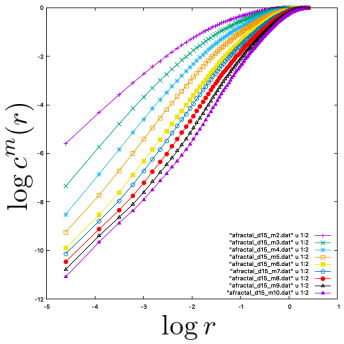

(a) DIV 15.

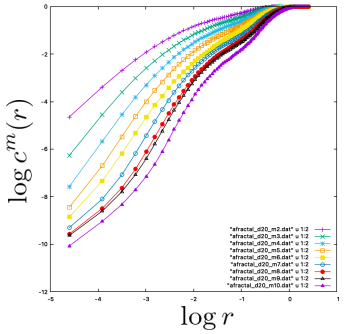

(b) DIV 20.

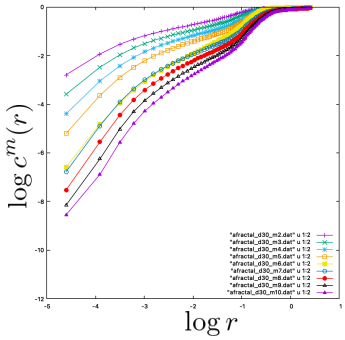

(c) DIV 30.

Fig. 6. Relationship between correlation integral and distance.

Next, the slope $V(m)$ is calculated from the graph in Fig. 6 and the relationship between the slope and the distance is shown in in Fig. 7. In general, the fractal dimension can be estimated from this graph. However, we can confirm that there are no clear scaling regions in any case of DIV. In particular, in the case of DIV15, the graph changes linearly as m increases. In the case of DIV 20 and 30, we can see how $V(m)$ is trying to converge in a certain region of $\log r$. In addition, the region where it is trying to converge is wider for DIV30.

From these results, it was not possible to derive fractal dimension values with the neuron signals used in this study. However, Fig. 7 suggests that the self-similarity feature increased as the number of days passed from DIV 15 to 30. In the future, we would like to propose a method to calculate these features.

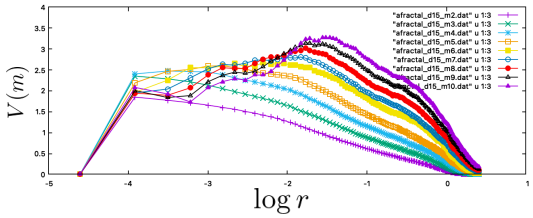

(a) DIV 15.

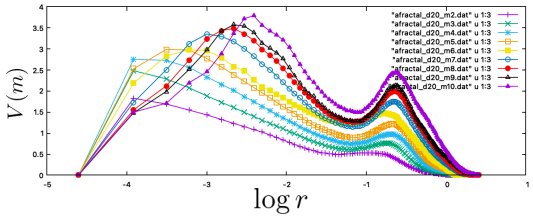

(b) DIV 20.

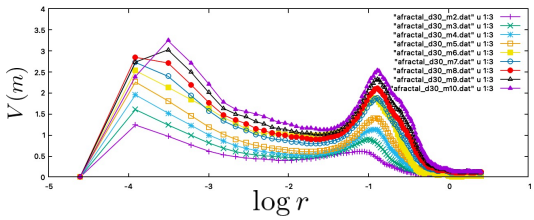

(c) DIV 30.

Fig. 7. Fractal dimension.

V. Discussion

In addition to self-similarity, chaos is characterized by the Lyapunov exponent as a dynamic feature. In a previous study we measured the Lyapunov exponent of neuronal signals and confirmed that all neuronal signals exhibit positive values, i.e., chaos [4]. In this study, the Lyapunov exponent was also calculated for the 3-minute neuron signal. The results are shown in the following table. As before, we confirmed that the Lyapunov exponents were positive in all cultures and that the Lyapunov exponents became smaller as the number of days passed.

TABLE I
Lyapunov exponent.

Neuron type	λ
DIV 15	3.89
DIV 20	3.38
DIV 30	2.76

The fractal dimension and Lyapunov exponent results indicate that the neuronal signal increases in self-similarity and weakens in orbital instability with growth.

VI. Conclusion

In this study, we investigated the characteristics of nonlinearity using attractor reconstruction and fractal dimension on actual neuronal signals. From the result of the attractor reconstruction, we confirm that young neurons are more complex and older neurons have grown to have some structure. The same can be said of the fractal dimension results. In other words, for young neurons (DIV 15), there were no scaling regions at all in the fractal dimension graphs, whereas for DIV 20 and 30, regions of attempted convergence were observed. However, the present approach did not provide a quantitative assessment of the chaotic properties of the neuronal signals.

As future work, we will apply the attractor reconstruction and fractal dimension to other cultures as well, since we were only able to apply it to one culture this time. We would like to propose a nonlinear method to clarify how chaotic characteristics of neuronal signals change with the growth process of the brain.

Acknowledgment

We would like to express our gratitude to MaxWell Biosystems for providing the real neuron data used in this research. Special thanks to Dr. Urs Frey and Dr. Marie Engelene J. Obien for their invaluable support and collaboration.

References

[1] M. Hruska-Plochan et al., "Human Neural Networks with Sparse TDP-43 Pathology Reveal NPTX2 Misregulation in ALS/FTLD," *bioRxiv*, doi: https://doi.org/10.1101/2021.12.08.471089, Sep. 2021.

[2] S. Ronchi, A. P. Buccino, G. Prack, S. S. Kumar, M. Schröter, M. Fiscella and A. Hierlemann, "Electrophysiological Phenotype Characterization of Human iPSC-Derived Neuronal Cell Lines by Means of High-Density Microelectrode Arrays," *Adv Biol (Weinh)*, doi: 10.1002/adbi.202000223, Jan. 2021.

[3] T. Kuroda, N. Matsuda, Y. Ishibashi and I. Suzuki, "Detection of Astrocytic Slow oscillatory Activity and Response to Seizurogenic Compounds using Planar Microelectrode Array," *Frontiers in Neuroscience*, https://doi.org/10.3389/fnins.2022.1050150, Jan. 2023.

[4] Y. Uwate, M. E. J. Obien, U. Frey and Y. Nishio, "Time Series Analysis of Neurons and Visualization of Network Characteristics," *2019 RISP International Workshop on Nonlinear Circuits, Communications and Signal Processing (NCSP2019)* , pp. 450-453, Mar. 2019.

[5] D. J. Bakkum U. Frey, M. Radivojevic, T. L. Russell, J. Mller, M. Fiscella and A. Hierlemann, "Tracking Axonal Action Potential Propagation on a High-Density Microelectrode Array Across Hundreds of Sites," *Nature Communications*, 4, 2181. http://doi.org/10.1038/ncomms3181, 2013.

[6] U. Frey, J. Sedivy, F.Heer, R. Pedron,M.Ballini, J. Mueller and A.Hierlemann, "Switch-Matrix-Based HighDensity Microelectrode Array in CMOS Technology," *IEEE Solid-State Circuits*, 45(2), 467482. http://doi.org/10.1109/JSSC.2009.2035196, 2010.

[7] M. E. J. Obien, K. Deligkaris, T. Bullmann, D. J. Bakkum, and U. Frey, "Revealing Neuronal Function through Microelectrode Array Recordings," *Frontiers in Neuroscience*, 8 (423). http://doi.org/10.3389/fnins.2014.00423, 2015.

[8] N. H. Packard, J. P. Crutchfield, J. D. Farmar and R. S. Shaw, "Geometry from a Time Series," *Physical Review Letters*, Vol. 45, No. 9, pp. 712-716, Sep. 1980.

[9] F. Takens, "Detecting Strange Attractors in Turbulence," *Lecture Notes in Mathematics*, Vol. 898, pp. 366-381, 1981.

[10] P. Grassberger and I. Procaccia, "Measuring the Strangeness of Strange Attractors," *Physica*, Vol. 9D, pp. 189-208, 1983.

[11] P. Grassberger and I. Pracassia, "Characterization of Strange Attractors," *Physical Review Letters*, Vol. 50, No. 3, pp. 346-349, 1983.